Facile fabrication of an efficient $BiVO_4$ thin film electrode for water splitting under visible light irradiation

Qingxin Jia[a], Katsuya Iwashina[a], and Akihiko Kudo[a,b,1]

[a]Department of Applied Chemistry, Faculty of Science, Tokyo University of Science, 1-3 Kagurazaka, Shinjuku-ku, Tokyo 162-8601, Japan; and [b]Division of Photocatalyst for Energy and Environment, Research Institute of Science and Technology, Tokyo University of Science, 2641 Noda-shi, Yamazaki, Chiba-ken 278-8510, Japan

Edited by Royce W. Murray, The University of North Carolina at Chapel Hill, Chapel Hill, NC, and approved April 25, 2012 (received for review March 17, 2012)

An efficient $BiVO_4$ thin film electrode for overall water splitting was prepared by dipping an F-doped SnO_2 (FTO) substrate electrode in an aqueous nitric acid solution of $Bi(NO_3)_3$ and NH_4VO_3, and subsequently calcining it. X-ray diffraction of the $BiVO_4$ thin film revealed that a photocatalytically active phase of scheelite-monoclinic $BiVO_4$ was obtained. Scanning electron microscopy images showed that the surface of an FTO substrate was uniformly coated with the $BiVO_4$ film with 300–400 nm of the thickness. The $BiVO_4$ thin film electrode gave an excellent anodic photocurrent with 73% of an IPCE at 420 nm at 1.0 V vs. Ag/AgCl. Modification with CoO on the $BiVO_4$ electrode improved the photoelectrochemical property. A photoelectrochemical cell consisting of the $BiVO_4$ thin film electrode with and without CoO, and a Pt counter electrode was constructed for water splitting under visible light irradiation and simulated sunlight irradiation. Photocurrent due to water splitting to form H_2 and O_2 was confirmed with applying an external bias smaller than 1.23 V that is a theoretical voltage for electrolysis of water. Water splitting without applying external bias under visible light irradiation was demonstrated using a $SrTiO_3$:Rh photocathode and the $BiVO_4$ photoanode.

hydrogen production | solar energy conversion | visible light response

The development of powdered photocatalysts and semiconductor photoelectrodes for water splitting have been studied extensively in view of utilization of solar energy, since the report of the Honda-Fujishima effect (1). There are advantageous and disadvantageous points for water splitting using the powdered photocatalysts and photoelectrochemical cells. Although a powdered photocatalyst system is simple, H_2 and O_2 are produced as a mixture. In contrast to it, photoelectrochemical cells give H_2 separately from O_2 gas. Moreover, even if powdered photocatalysts do not possess band potentials suitable for water splitting (the bottom of the conduction band <0 V and the top of the valence band >1.23 V vs. NHE at pH 0), water splitting may be achieved by application of these powdered photocatalysts to photoelectrodes with applying some external bias. However, the electrical conductivity of semiconductor electrode is indispensable, resulting in that the number of the photoelectrode materials is limited.

It has been reported that many metal oxides are active photocatalysts for water splitting into H_2 and O_2 stoichiometrically under UV light irradiation (2). Photoelectrodes, such as TiO_2 (1, 3, 4), $SrTiO_3$ (5, 6), $BaTiO_3$ (7), and $KTaO_3$ (8) have been reported for photoelectrochemical water splitting under UV light irradiation. Development of a photoelectrode material with visible light response has been sought for efficient utilization of solar energy. It has been reported that Fe_2O_3 (9–11), WO_3 (12–14), $BiVO_4$ (15–24), and $SrTiO_3$:Rh (25) of metal oxide electrodes respond to visible light. Recently, some (oxy) nitride materials such as TaON (26, 27), Ta_3N_5 (27, 28), $SrNbO_2N$ (29), and $Ta_{0.9}Co_{0.1}N_x$ (30) have also been found to be visible light responsive photoelectrodes for water splitting.

$BiVO_4$ has three crystal systems: Scheelite structure with monoclinic (s-m) and tetragonal (s-t) phases, and zircon structure with tetragonal (z-t) phase (31–34). Among them, the scheelite monoclinic $BiVO_4$ shows the highest photocatalytic activity for O_2 evolution from an aqueous $AgNO_3$ solution under visible light irradiation (19, 34–36). However, $BiVO_4$-powdered photocatalyst is inactive for overall water splitting into H_2 and O_2, because the bottom of conduction band is more positive than the reduction potential of H_2O to form H_2. $BiVO_4$, with an n-type semiconductor character, shows an excellent photoelectrochemical property (15). The photoelectrochemical cell consisting of $BiVO_4$ can split water under visible light irradiation (16, 19). There are mainly two methods for the preparation of $BiVO_4$ electrodes: $BiVO_4$ powder-loaded electrodes and $BiVO_4$-coated electrodes using metal organic precursors. The $BiVO_4$ photoelectrode prepared by the metal-organic decomposition method gives 20% of IPCE at 420 nm with applying 0.6 V vs. Ag/AgCl for water splitting (15). It also works with 1.6 V of an externally applied bias vs. a counter electrode (C.E.) under visible light irradiation (16). A $BiVO_4$ photocatalyst electrode that is readily prepared by pasting $BiVO_4$ nanoparticle prepared in an acetic acid onto an FTO substrate can split water with an externally applied bias smaller than 1.23 V vs. a Pt counter electrode under simulated sunlight irradiation (19). It is important to develop a simple and large-scale producible preparation method for the photoelectrode.

Surface modification is a useful method to improve photoelectrochemical properties. Modification with Co_3O_4 by precipitation method increases the photocurrent of $BiVO_4$ electrode (18). Recently, cobalt phosphate (CoPi) prepared by an electrodeposition has been reported as an oxygen evolving electrocatalyst (37). Photoelectrochemical properties of Si (37, 38), Fe_2O_3 (39–41), WO_3 (42), $BiVO_4$ (43, 44), and $BiVO_4$ doped with Mo and W (45, 46) electrodes are improved with the surface modification with the CoPi cocatalyst. Modification with FeOOH is also effective (47).

In the present study, we developed a facile fabrication of an efficient $BiVO_4$ thin film coated on FTO electrode using inorganic salts of bismuth and vanadium. The formation mechanism of the present $BiVO_4$ thin film electrode was discussed. Photoelectrochemical property of the obtained $BiVO_4$ thin film electrode with and without surface modification with cobalt oxide was examined. Water splitting was also demonstrated using photoelectrochemical cells consisting of a Pt counter electrode or a

Author contributions: A.K. designed research; Q.J. and K.I. performed research; and Q.J. and A.K. wrote the paper.

The authors declare no conflict of interest.

This article is a PNAS Direct Submission.

[1]To whom correspondence should be addressed. E-mail: a-kudo@rs.kagu.tus.ac.jp.

This article contains supporting information online at www.pnas.org/lookup/suppl/doi:10.1073/pnas.1204623109/-/DCSupplemental.

$SrTiO_3$: Rh photocathode under visible light and simulated sunlight irradiation.

Results and Discussion

Preparation of $BiVO_4$ Thin Film Electrode. Fig. 1 shows XRD patterns of the obtained $BiVO_4$ thin film electrodes prepared under different condition. The diffraction pattern of $BiVO_4$ (s-m) was observed for the sample calcined at 673 K for 2 h after drying an FTO substrate treated with an aqueous nitric acid precursor solution dissolving $Bi(NO_3)_3$ and NH_4VO_3, in addition to the XRD pattern of SnO_2 derived from the FTO substrate (Fig. 1*A*). Thus, $BiVO_4$ thin film with scheelite structure with monoclinic phase (s-m) that showed high photocatalytic activity was obtained by this simple preparation method. The crystal structure of $BiVO_4$ thin films prepared at various calcination temperatures was examined (Fig. 1 *B–E*). A soda-lime glass was used as a substrate for these XRD measurements, because the (002) diffraction peak of $BiVO_4$ was overlapped with the (101) diffraction peak of FTO. $BiVO_4$ (s-m) was obtained by calcination at 573 and 623 K as a major component, in addition to a minor product of zircon structure tetragonal phase $BiVO_4$ (z-t). A single phase of $BiVO_4$ (s-m) was obtained by calcination at 673 and 723 K. Fig. 2 shows SEM images of surface and cross-section of $BiVO_4$ thin films prepared at various calcination temperatures. An FTO substrate without the $BiVO_4$ thin film was treated with 2 mmol L^{-1} of an aqueous nitric acid solution and subsequently calcined at 673 K for 2 h as a reference sample (Fig. 2*A*). It was observed that an FTO substrate was dense aggregates of crystal with bumpy surface. The morphologies of the $BiVO_4$ thin films changed with calcination temperature. The thin film without calcination was sponge-like and orange. Calcination at 573 K gave network structure for the thin film. The thin film began to sinter by calcination at 623 K and became dense and porous by calcination at 673 K. The cross-sectional image revealed that the thickness of the $BiVO_4$ porous film was several hundred nanometers. This morphology was quite different from that of powder-loaded electrodes (19). These network and porous structures were considered to be formed by volatilization of water and HNO_3, and decomposition of some by-products, during the calcination as mentioned later. The thin film considerably sintered to form necked nano-particles by calcination at 723 K. Thus, this simple preparation method gave a porous $BiVO_4$ (s-m) thin film well attached on the FTO substrate. UV-vis. transmission spectra of $BiVO_4$ thin films showed that the thickness was controllable by changing the concentration (20–300 mmol L^{-1}) of $Bi(NO_3)_3$ and NH_4VO_3 dissolving in an aqueous nitric acid precursor solution as shown in Fig. S1. The wavy spectra observed in the wavelength range of 500–800 nm was due to light interference.

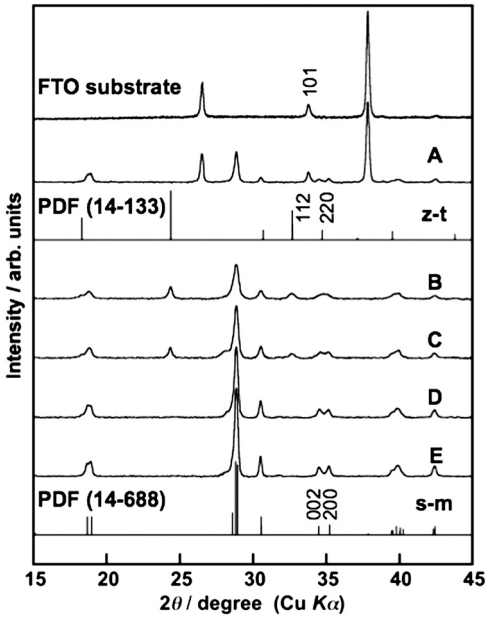

Fig. 1. X-ray diffraction patterns of $BiVO_4$ thin films formed on (*A*) FTO and (*B–E*) soda-lime glass substrates. Preparation conditions, calcined at (*B*) 573 K, (*C*) 623 K, (*A*, *D*) 673 K, and (*E*) 723 K for 2 h.

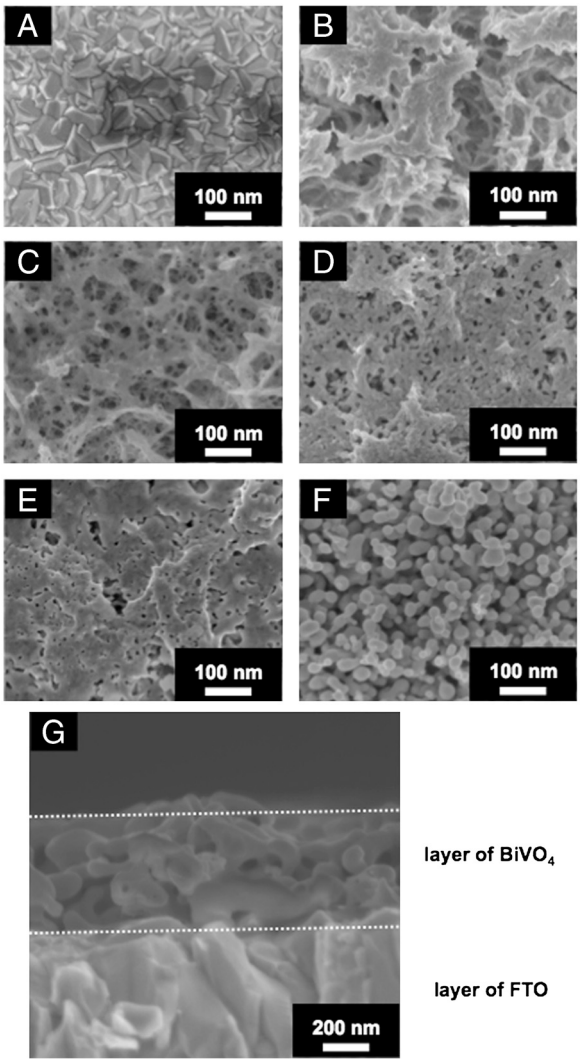

Fig. 2. Scanning electron microscope images of (*A*) FTO substrate, (*B–F*) surface and (*G*) cross-section of $BiVO_4$ thin film electrodes. Preparation conditions, (*B*) dried and calcined at (*C*) 573 K, (*D*) 623 K, (*E*, *G*) 673 K, and (*F*) 723 K for 2 h.

Mechanism of Formation of $BiVO_4$ Thin Film. The formation process of $BiVO_4$ thin films from an aqueous nitric acid precursor solution containing $Bi(NO_3)_3$ and NH_4VO_3 was examined with XPS and TG. The precursor solution covered on an FTO substrate became an orange film after drying, and a bright yellow film after calcination. The chemical state of the orange film was examined by XPS and TG-DTA. XPS spectra of each element of the orange film were different from those of the $BiVO_4$ thin film as shown in Fig. 3. The binding energies of $Bi4f_{7/2}$ (159.0 eV), $V2p_{3/2}$ (516.7 eV), and O1s (529.7 eV) of the $BiVO_4$ thin film calcined at 673 K were coincident with literature's data of $BiVO_4$ (s-m) (48, 49). The deconvoluted O1s peak at 531.6 eV was assigned to surface hydroxyl groups (50, 51). NO_3^- was almost decomposed by the calcination. Binding energies of Bi4f (159.5 eV) and V2p (517.5 eV) of the orange film without calcination were larger than

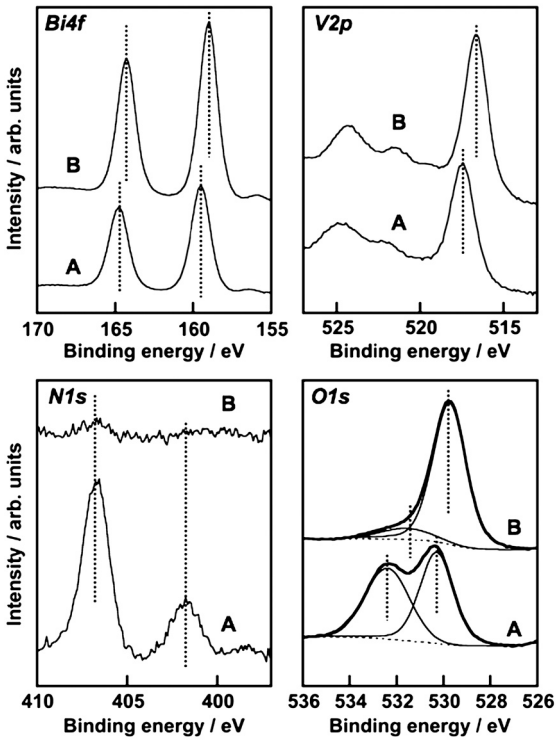

Fig. 3. X-ray photoelectron spectra of $BiVO_4$ thin film electrode. (*A*) Before and (*B*) after calcination at 673 K for 2 h.

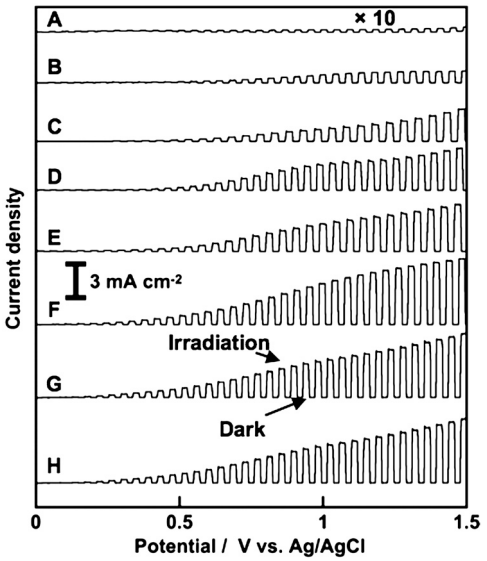

Fig. 4. Current vs. potential curves of $BiVO_4$ thin film electrodes under visible light irradiation. Concentration of precursor solution and calcination temperature, (*A*) 200 mmol L^{-1}, 573 K, (*B*) 200 mmol L^{-1}, 623 K, (*C*) 20 mmol L^{-1}, 673 K, (*D*) 50 mmol L^{-1}, 673 K, (*E*) 100 mmol L^{-1}, 673 K, (*F*) 200 mmol L^{-1}, 673 K, (*G*) 300 mmol L^{-1}, 673 K, and (*H*) 200 mmol L^{-1}, 723; calcination time, 2 h. Electrolyte, 0.1 mmol L^{-1} of an aqueous K_2SO_4 solution; sweep rate, 20 mV s^{-1}; light source, 300 W Xe-lamp with a cut-off filter ($\lambda > 420$ nm).

those of the calcined $BiVO_4$ thin film, whereas they were close to those of $(BiO)_2Cr_2O_7$ at 159.8 eV (52) and $NaVO_3$ at 517.0 eV (53), respectively. It suggested that Bi and V in the orange film took the chemical states similar to $[BiO]^+$ and $[VO_3]^-$ species, respectively. The XPS spectra of N1s at 401.8 eV and 406.7 eV were assigned to NH_4^+ and NO_3^- (54), respectively. The O1s peak at 532.4 eV well agreed with that of NO_3^- in NH_4NO_3 (532.5 eV) (54). These results indicated that $[BiO]^+$, VO_3^-, NO_3^-, and NH_4^+ were contained in the orange film before calcination. TG-DTA measurement was carried out to examine the formation temperature of the $BiVO_4$ thin film from these chemical species as shown in Fig. S2. Significant loss of weight was observed around 480 K accompanied with an exothermic process and a subsequent endothermic process. This exothermic process was probably due to the chemical reaction heat of $[BiO]^+$ with VO_3^- to form $BiVO_4$. The loss of weight with the endothermic process was mainly caused by the decomposition of NH_4NO_3 to release N_2O and NH_3 gases (55). These results led the formation process of the $BiVO_4$ thin film as shown in Fig. S3. When $Bi(NO_3)_3$ of a starting material was dissolved in an aqueous nitric acid solution, $[BiO]^+$ and NO_3^- species formed (56). The bright yellow color of the precursor solution suggested the existence of VO_2^+ species that was formed from VO_3^- under a strongly acidic condition (57). VO_2^+ species changed to VO_3^- after drying, and these chemical species turned into NH_4NO_3 and $[BiO]^+[VO_3]^-$. Calcination above 480 K caused the decomposition of NH_4NO_3 and the reaction of $[BiO]^+[VO_3]^-$ to form $BiVO_4$. Porous structure of the thin film observed by SEM (Fig. 2*C*) formed accompanied with running out of gaseous products.

Photoelectrochemical Property of $BiVO_4$ Thin Film Electrode. Effects of calcination temperature and film thickness on photoelectrochemical properties of $BiVO_4$ thin films were examined as shown in Fig. 4. $BiVO_4$ thin film electrodes calcined at different temperatures gave anodic photocurrents under visible light irradiation. The anodic photocurrent increased as the calcination temperature was raised. The photocatalytic activity of the $BiVO_4$ (z-t) powder was lower than that of $BiVO_4$ (s-m) for O_2 evolution from an aqueous $AgNO_3$ solution under visible light irradiation (35). The thin film containing $BiVO_4$ (z-t) calcined at 573 and 623 K gave relatively small photocurrents corresponding to the photocatalytic property. The thin film electrodes with a single phase of $BiVO_4$ (s-m) calcined at 673–723 K showed large photocurrents. The increase in the anodic photocurrent with the increase in the calcination temperature was due to the improvement of the denseness of the thin film as observed by SEM, and the purity and crystallinity of scheelite-monoclinic phase as confirmed by XRD. On the other hand, as the thickness of the $BiVO_4$ film was increased, the anodic photocurrent became large. The $BiVO_4$ thin film prepared using 200–300 mmol L^{-1} of precursor solutions gave an excellent photoelectrochemical property. Thicknesses of these thin films were sufficient for light absorption. These results concluded that the optimum calcination temperature and the concentration of the precursor solution were 673–723 K and 200–300 mmol L^{-1}, respectively. Fig. 5 shows action spectra of the optimized $BiVO_4$ thin film electrode. The onset of the IPCE agreed well with that of an absorption edge of

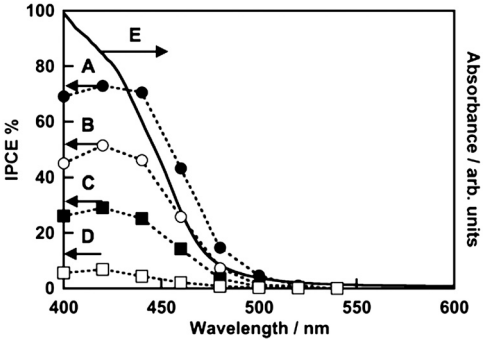

Fig. 5. (*A–D*) Action spectra and (*E*) a diffuse reflection spectrum of $BiVO_4$ thin film electrode. Preparation condition, calcined at 673 K for 2 h. Electrolyte, 0.1 mmol L^{-1} of an aqueous K_2SO_4 solution; potential, (*A*) 1 V, (*B*) 0.8 V, (*C*) 0.6 V, and (*D*) 0.4 V vs. Ag/AgCl.

$BiVO_4$. This result indicated that the anodic photocurrent attributed to the band gap transition from the valence band of hybrid Bi6s-O2p orbitals to the conduction band of V3d (35). IPCE increased with an increase in the electrode potential. The $BiVO_4$ thin film electrode gave an excellent anodic photocurrent with 73% of an IPCE at 420 nm at 1 V vs. Ag/AgCl. Modification with cobalt oxide on the $BiVO_4$ electrode improved the photoelectrochemical property as previously reported (43, 45, 46). The onset potential of the anodic photocurrent for the cobalt oxide-modified $BiVO_4$ electrode was more negative than that for the nonmodified electrode as shown in Fig. S4. This result indicated that the loaded cobalt oxide improved the photoelectrochemical performance of the $BiVO_4$ thin film electrode. XPS was carried out to examine the chemical state of the cobalt oxide loaded on the $BiVO_4$ thin film electrode. Fig. S5 shows the Co2p and P2p spectra of cobalt oxide-modified $BiVO_4$ electrode before and after photoelectrochemical water splitting. The XPS spectra of Co2p at 780.1 eV accompanied with the satellite were assigned to Co^{2+} in CoO. The peak of P2p was not detected, suggesting that the cobalt compound should be CoO. An average ratio of Co to Bi was estimated to be about 1:1 by XPS.

Photoelectrochemical Overall Water Splitting. It is important to see the stability of photocurrent and to determine the amounts of evolved H_2 and O_2 for photoelectrochemical water splitting, because we cannot always guarantee that obtained photocurrent is due to water splitting. Fig. 6 shows photoelectrochemical water splitting using a $BiVO_4$ thin film (1.5 cm^2) with 1.0 V of an applied potential vs. Ag/AgCl. Steady photocurrent was obtained after 30 minutes and the rate of H_2 evolution agreed well with the photocurrent (Fig. 6*B*). H_2 and O_2 evolved in a stoichiometric ratio from Pt and $BiVO_4$ electrodes, respectively. The amount of H_2 evolved was similar to the half of the amount of electron passing through the outer circuit (Fig. 6*A*). This result indicated that the observed photocurrent was due to water splitting. Photoelectrochemical water splitting was also examined using a solar simulator (AM1.5) with applying an external bias smaller than 1.23 V that was a theoretical voltage required for electrolysis of water in order to see if the present photoelectrochemical cell consisting of $BiVO_4$ thin film and Pt electrodes works for solar energy conversion as shown in Fig. 7*A*. The solar energy conversion efficiency was estimated to be 0.005% with applying an external bias at 1 V vs. C.E. Large photocurrent was obtained for the CoO-modified $BiVO_4$ thin film even applying a smaller external bias (0.6 V vs. C.E.) as shown in Fig. 7*B*. The solar energy conversion efficiency was estimated to be 0.04% with 0.6 V vs. C.E.

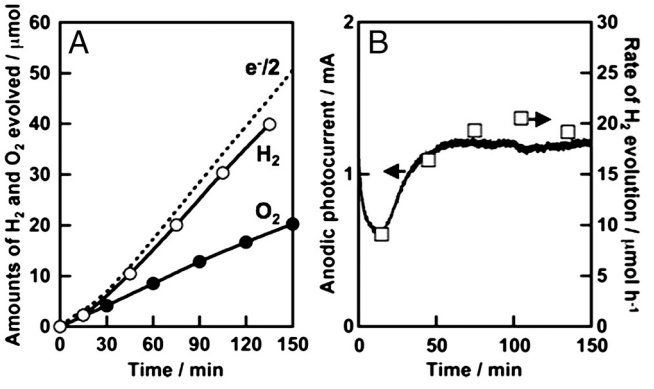

Fig. 6. (*A*) Photoelectrochemical overall water splitting over $BiVO_4$ thin film electrode and (*B*) stability of photocurrent using $BiVO_4$ thin film electrode and Pt counter under visible light irradiation. Dashed line: the half of the amount of electron, open square: the rate of H_2 evolution. Preparation condition, calcined at 673 K for 2 h. Electrolyte, 0.1 mmol L^{-1} of an aqueous K_2SO_4 solution; potential, 1 V vs. Ag/AgCl; electrode area, 1.5 cm^2; light source, 300 W Xe-lamp with a cut-off filter ($\lambda > 420$ nm).

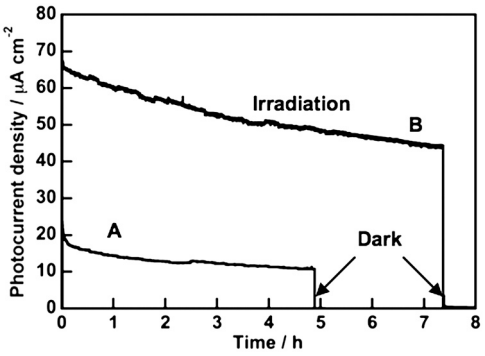

Fig. 7. Stability of photocurrents of (*A*) $BiVO_4$ and (*B*) CoO-modified $BiVO_4$ thin film electrodes under simulated sunlight irradiation (AM1.5). Preparation condition, calcined at 673 K for 2 h. Electrolyte, 0.1 mmol L^{-1} of an aqueous K_2SO_4 solution (phosphate buffer, pH = 6.9); applied voltage, (*A*) 1 V, (*B*) 0.6 V vs. C.E.

A photoelectrochemical cell consisting of a $SrTiO_3$:Rh (7%) photocathode (25) and the present $BiVO_4$ thin film photoanode was constructed for water splitting. Photoelectrochemical water splitting proceeded under visible light irradiation with applying non-bias, as shown in Fig. 8. Steady photocurrent was obtained and the rate of H_2 evolution agreed well with the photocurrent (Fig. 8*B*). H_2 and O_2 evolved in a stoichiometric ratio on the $SrTiO_3$:Rh and $BiVO_4$ electrodes, respectively. The amount of H_2 evolved was similar to the half of the amount of electron passing through the outer circuit (Fig. 8*A*). Thus, we succeeded in constructing a photoelectrochemical cell consisting of metal oxide materials for water splitting without applying an external bias.

In summary, we have developed a facile fabrication of an efficient $BiVO_4$ thin film electrode for overall water splitting from an aqueous nitric acid solution of $Bi(NO_3)_3$ and NH_4VO_3. It was revealed that the chemical species contained in the starting materials reacted with each other to form $BiVO_4$ (s-m) via $BiVO_4$ (z-t) by calcination. The $BiVO_4$ (s-m) electrode showed a larger anodic photocurrent than $BiVO_4$ (z-t). This was consistent with the order in an activity of powdered $BiVO_4$ photocatalyst for O_2 evolution from an aqueous $AgNO_3$ solution under visible light irradiation. Anodic photocurrent of the $BiVO_4$ thin film electrode depended on the concentration of a precursor solution and calcination temperature. The $BiVO_4$ thin film electrode prepared at 673–723 K using 200–300 mmol L^{-1} of the precursor solution gave an excellent anodic photocurrent with 73% of an IPCE at 420 nm at 1 V vs. Ag/AgCl. Photoelectrochemical water splitting using the $BiVO_4$ thin film proceeded with applying an external

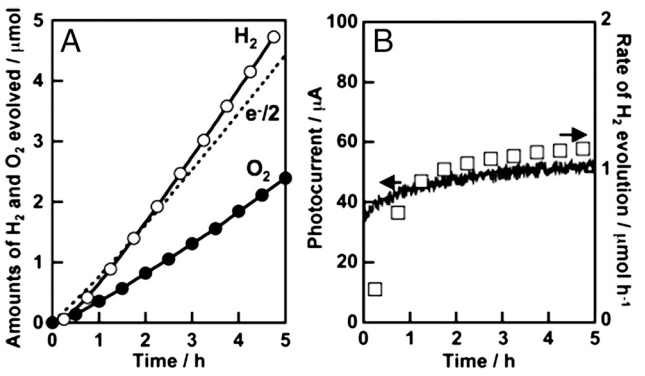

Fig. 8. (*A*) Photoelectrochemical overall water splitting and (*B*) stability of photocurrent using $BiVO_4$ thin film electrode and $SrTiO_3$:Rh photocatalyst electrode under visible light irradiation. Dashed line: the half of the amount of electron, open square: the rate of H_2 evolution. Electrolyte, 0.1 mmol L^{-1} of an aqueous K_2SO_4 solution; applied voltage, 0 V; electrode area, 4 cm^2 each; light source, 300 W Xe-lamp with a cut-off filter ($\lambda > 420$ nm).

bias smaller than 1.23 V, which is a theoretical voltage required for electrolysis of water. The amount of H_2 evolved was similar to the half of the amount of electron passing through the outer circuit, indicating that the photocurrent was due to water splitting. Modification with CoO on the $BiVO_4$ electrode improved the photoelectrochemical property. The metal oxide photoelectrochemical system was constructed for water splitting under visible light irradiation with applying no external bias employing a $SrTiO_3$:Rh photocathode and the $BiVO_4$ thin film photoanode.

Materials and Methods

Preparation of $BiVO_4$ Thin Film and $SrTiO_3$:Rh Electrodes. When 0.2–3 mmol of $Bi(NO_3)_3$ (Kanto Chemical; 99.9%) and NH_4VO_3 (Kanto Chemical; 99.0%) at an equal molar ratio was dissolved in 10 mL of an aqueous nitric acid solution (2 mol L^{-1}), a yellow precursor solution was obtained. An FTO (F-doped SnO_2) transparent substrate electrode (AGC Fabritech; A-110U80, sheet resistance: 20 $\Omega\,sq^{-1}$) was dipped in the precursor solution for 1–2 s. Then, the FTO substrate was covered with the yellow liquid of the precursor solution. After dryness at room temperature, an orange film was obtained on the FTO. Calcination of this film at 573–723 K for 2 h in air gave a yellow $BiVO_4$ thin film. Cobalt oxide cocatalyst was loaded on the $BiVO_4$ film with an area of 2.5 cm^2 by an impregnation method with calcination at 673 K for 1 h in air using an aqueous solution (5 μL, 80 mmol L^{-1}) of $Co(NO_3)_2$ (Wako Pure Chemical; 99.5%), if necessary (17, 18).

$SrTiO_3$ powder doped with 7 mol% of Rh to a Ti site was prepared by a solid state reaction in order to obtain a photocathode for the construction of a photoelectrochemical cell (25). Starting materials, $SrCO_3$ (Kanto Chemical; 99.9%), TiO_2 (Soekawa Chemical; 99.9%), and Rh_2O_3 (Wako Pure Chemical) were mixed with the ratio of Sr:Ti:Rh = 1.07:0.93:0.07. The mixture was calcined in air at 1,173 K for 1 h and then at 1,373 K for 10 h in an alumina crucible. $SrTiO_3$:Rh photocatalyst electrodes were prepared by coating the paste composed of 20 mg of $SrTiO_3$:Rh photocatalyst powders, 20 μL of acetylacetone (Kanto Chemical; 99.5%), and 40 μL of distilled water on an indium tin oxide (ITO) transparent electrode and then calcining at 573 K for 2 h in air (25).

Characterization. The crystal form of obtained $BiVO_4$ thin film was confirmed by X-ray diffraction (Rigaku; miniFlex). Diffuse reflectance spectra were obtained using a UV-vis-NIR spectrometer (Jasco; Ubest-570) and were converted from reflection to absorbance by the Kubelka-Munk method, if necessary. The formation process of the $BiVO_4$ thin film from the precursor solution were examined using a thermobalance (Ulvac; TGD-9600) for thermogravimetric–differential thermal analyses (TG-DTA) and an X-ray photoelectron spectrometer (Jeol; JPS-9010MC) with a Mg Kα (1253.6 eV) target. Obtained XPS spectra were corrected by C1s of adventitious carbon (284.6 eV). The morphology of obtained $BiVO_4$ thin films was observed by scanning electron microscopy (Jeol; JSM-6700F).

Photoelectrochemical Measurement. Photoelectrochemical properties were evaluated using a potentiostat (Hokuto Denko; HZ-5000 or HSV-100) with a three-electrode H-type cell divided into working and counter electrode compartments by Nafion 117 (DuPont). The $BiVO_4$ thin film electrode, a Pt electrode, and a saturated Ag/AgCl electrode (DKK TOA; HS-205C) were used as working, counter, and reference electrodes, respectively. A $SrTiO_3$:Rh electrode was also employed as a photocathode (25). 0.1 mol L^{-1} of an aqueous K_2SO_4 (Kanto Chemical; 99.0%) solution was used as an electrolyte. An aqueous phosphate buffer solution [0.025 mol L^{-1} of KH_2PO_4 (Kanto Chemical; 99.6%) +0.025 mol L^{-1} of Na_2HPO_4 (Kanto Chemical; 99.5%)] was employed to adjust the pH to 6.9, if necessary.

Photoelectrochemical water splitting was carried out in an Ar gas flow system at 10 mL min^{-1} of a flow rate. The amounts of evolved gases were determined with gas chromatography (Shimadzu; MS-5A column, Ar carrier, TCD). The light source was a 300 W Xe-lamp (PerkinElmer; Cermax- PE300BF). Wavelength of the incident light was controlled by cut-off filters (HOYA), an NIR-absorbing filter (Sigma Koki; CCF-50S-500C), and a Plano convex lens (Sigma Koki; SLSQ- 60-150P). The working electrode was irradiated with light from an FTO side. The electrolytes in both compartments were bubbled with N_2 or Ar before measurements for removal of dissolved O_2. A 300 W Xe-lamp (Ashahi Spectra; MAX-301) with band-pass filters was employed for IPCE measurement. The number of incident photons was measured using a photodiode head (OPHIRA; PD300-UV) and a power monitor (NOVA). IPCE was calculated according to Eq. **1**.

$$\mathrm{IPCE\%} = \frac{1240 \times [\text{Photocurrent density}/\mu\mathrm{A\,cm^{-2}}]}{[\text{Wavelength}/\mathrm{nm}] \times [\text{Photo flux}/\mathrm{W\,m^{-2}}]} \times 100 \quad \textbf{[1]}$$

A solar simulator (Peccell Technologies; PEC-L11, 100 mW cm^{-2}) was employed for solar energy conversion determined by Eq. **2**.

$$\begin{aligned}\text{Solar energy conversion efficiency\%} &= \frac{[\Delta G^0(\mathrm{H_2O})/\mathrm{J\,mol^{-1}}] \times \frac{1.23\text{-}E_{apply}/V}{1.23} \times [\text{Rate of } \mathrm{H_2} \text{ evolution}/\mathrm{mol\,h^{-1}}]}{3600 \times [\text{Solar energy(AM-1.5)}/\mathrm{W\,cm^{-2}}] \times [\text{Dimension of electrodes}/\mathrm{cm^2}]} \times 100 \\ &= \frac{[\text{Photocurrent density}/\mathrm{mA\,cm^{-2}}] \times [1.23\text{-}E_{apply}/V]}{[\text{Solar energy (AM-1.5)}/\mathrm{mW\,cm^2}]} \times 100 \quad \textbf{[2]}\end{aligned}$$

E_{apply} represents of the applied external bias between working and Pt counter electrodes.

ACKNOWLEDGMENTS. This work was supported by Toyota Motor Corporation.

1. Fujishima A, Honda K (1972) Electrochemical photolysis of water at a semiconductor electrode. *Nature* 238:37–38.
2. Kudo A, Miseki Y (2009) Heterogeneous photocatalyst materials for water splitting. *Chem Soc Rev* 38:253–278.
3. Yoneyama H, Sakamoto H, Tamura H (1975) Photo-electrochemical cell with production of hydrogen and oxygen by a cell reaction. *Electrochim Acta* 20:341–345.
4. Nozic AJ (1976) *p-n* photoelectrolysis cells. *Appl Phys Lett* 29:150–153.
5. Watanabe T, Fujishima A, Honda K (1976) Photoelectrochemical reactions at $SrTiO_3$ single-crystal electrode. *Bull Chem Soc Jpn* 49:355–358.
6. Wrighton MS, et al. (1976) Strontium-titanate photoelectrodes-efficient photoassisted electrolysis of water at zero applied potential. *J Am Chem Soc* 98:2774–2779.
7. Kennedy JH, Frese KW (1976) Photooxidation of water at barium-titanate electrodes. *J Electrochem Soc* 123:1683–1686.
8. Ellis AB, Kaiser SW, Wrighton MS (1976) Semiconducting potassium tantalate electrodes—Photoassistance agents for efficient electrolysis of water. *J Phys Chem* 80:1325–1328.
9. Lindgren T, et al. (2002) Aqueous photoelectrochemistry of hematite nanorod array. *Sol Energy Mater Sol Cells* 71:231–243.
10. Sivula K, Le Formal F, Grätzel M (2011) Solar water splitting: progress using hematite (alpha-Fe_2O_3) photoelectrodes. *Chem Sus Chem* 4:432–449.
11. Duret A, Grätzel M (2005) Visible light-induced water oxidation on mesoscopic alpha-Fe_2O_3 films made by ultrasonic spray pyrolysis. *J Phys Chem B* 109:17184–17191.
12. Spichigerulmann M, Augustynski J (1983) Aging effects in N-type semiconducting WO_3 films. *J Appl Phys* 54:6061–6064.
13. Alexander BD, Kulesza PJ, Rutkowska L, Solarska R, Augustynski J (2008) Metal oxide photoanodes for solar hydrogen production. *J Mater Chem* 18:2298–2303.
14. Miseki Y, Kusama H, Sugihara H, Sayama K (2010) Cs-modified WO_3 photocatalyst showing efficient solar energy conversion for O_2 production and Fe (III) ion reduction under visible light. *J Phys Chem Lett* 1:1196–1200.
15. Sayama K, et al. (2003) Photoelectrochemical decomposition of water on nanocrystalline $BiVO_4$ film electrodes under visible light. *Chem Commun* 2908–2909.
16. Sayama K, et al. (2006) Photoelectrochemical decomposition of water into H_2 and O_2 on porous $BiVO_4$ thin-film electrodes under visible light and significant effect of Ag ion treatment. *J Phys Chem B* 110:11352–11360.
17. Long MC, Beranek R, Cai WM, Kisch H (2008) Hybrid semiconductor electrodes for light-driven photoelectrochemical switches. *Electrochim Acta* 53:4621–4626.
18. Long MC, Cai WM, Kisch H (2008) Visible light induced photoelectrochemical properties of n-$BiVO_4$ and n-$BiVO_4$/p-CO_3O_4. *J Phys Chem C* 112:548–554.
19. Iwase A, Kudo A (2010) Photoelectrochemical water splitting using visible-light-responsive $BiVO_4$ fine particles prepared in an aqueous acetic acid solution. *J Mater Chem* 20:7536–7542.

20. Ye H, Lee J, Jang JS, Bard AJ (2010) Rapid screening of $BiVO_4$-based photocatalysts by scanning electrochemical microscopy (SECM) and studies of their photoelectrochemical properties. *J Phys Chem C* 114:13322–13328.
21. Berglund SP, Flaherty DW, Hahn NT, Bard AJ, Mullins CB (2011) Photoelectrochemical oxidation of water using nanostructured $BiVO_4$ films. *J Phys Chem C* 115:3794–3802.
22. Sayama K, et al. (2010) Effect of carbonate ions on the photooxidation of water over porous $BiVO_4$ film photoelectrode under visible light. *Chem Lett* 39:17–19.
23. Ng YH, Iwase A, Kudo A, Amal R (2010) Reducing graphene oxide on a visible-light $BiVO_4$ photocatalyst for an enhanced photoelectrochemical water splitting. *J Phys Chem Lett* 1:2607–2612.
24. Ye H, Park HS, Bard AJ (2011) Screening of electrocatalysts for photoelectrochemical water oxidation on W-doped $BiVO_4$ photocatalysts by scanning electrochemical microscopy. *J Phys Chem C* 115:12464–12470.
25. Iwashina K, Kudo A (2011) Rh-doped $SrTiO_3$ photocatalyst electrode showing cathodic photocurrent for water splitting under visible-ight irradiation. *J Am Chem Soc* 133:13272–13275.
26. Abe R, Higashi M, Domen K (2010) Facile fabrication of an efficient oxynitride TaON photoanode for overall water splitting into H_2 and O_2 under visible light irradiation. *J Am Chem Soc* 132:11828–11829.
27. Higashi M, Domen K, Abe R (2011) Fabrication of efficient TaON and Ta_3N_5 photoanodes for water splitting under visible light irradiation. *Energy Environ Sci* 4:4138–4147.
28. Ishikawa A, Takata T, Kondo JN, Hara M, Domen K (2004) Electrochemical behavior of thin Ta_3N_5 semiconductor film. *J Phys Chem B* 108:11049–11053.
29. Maeda K, Higashi M, Siritanaratkul B, Abe R, Domen K (2011) $SrNbO_2N$ as a water-splitting photoanode with a wide visible-light absorption band. *J Am Chem Soc* 133:12334–12337.
30. Cong YQ, et al. (2012) Tantalum cobalt nitride photocatalysts for water oxidation under visible light. *Chem Mater* 24:579–586.
31. Lim AR, Choh SH, Jang MS (1995) Prominent ferroelastic domain walls in $BiVO_4$ crystal. *J Phys: Condens Matter* 7:7309–7323.
32. Bierlein JD, Sleight AW (1975) Ferroelasticity in $BiVO_4$. *Solid State Commun* 16:69–70.
33. Hirota K, Komatsu G, Yamashita M, Takemura H, Yamaguchi O (1992) Formation, characterization and sintering of alkoxy-derived bismuth vanadate. *Mater Res Bull* 27:823–830.
34. Tokunaga S, Kato H, Kudo A (2001) Selective preparation of monoclinic and tetragonal $BiVO_4$ with scheelite structure and their photocatalytic properties. *Chem Mater* 13:4624–4628.
35. Kudo A, Omori K, Kato H (1999) A novel aqueous process for preparation of crystal form-controlled and highly crystalline $BiVO_4$ powder from layered vanadates at room temperature and its photocatalytic and photophysical properties. *J Am Chem Soc* 121:11459–11467.
36. Iwase A, Kato H, Kudo A (2010) A simple preparation method of visible-light-driven $BiVO_4$ photocatalysts from oxide starting materials (Bi_2O_3 and V_2O_5) and their photocatalytic activities. *J Sol Energ Eng* 132:021106.
37. Kanan MW, Nocera DG (2008) In situ formation of an oxygen-evolving catalyst in neutral water containing phosphate and Co^{2+}. *Science* 321:1072–1075.
38. Pijpers JJH, Winkler MT, Surendranath Y, Buonassisi T, Nocera DG (2011) Light-induced water oxidation at silicon electrodes functionalized with a cobalt oxygen-evolving catalyst. *Proc Natl Acad Sci USA* 108:10056–10061.
39. Barroso M, et al. (2011) The role of cobalt phosphate in enhancing the photocatalytic activity of alpha-Fe_2O_3 toward water oxidation. *J Am Chem Soc* 133:14868–14871.
40. McDonald KJ, Choi KS (2011) Photodeposition of co-based oxygen evolution catalysts on alpha-Fe_2O_3 photoanodes. *Chem Mater* 23:1686–1693.
41. Zhong DK, Cornuz M, Sivula K, Graetzel M, Gamelin DR (2011) Photo-assisted electrodeposition of cobalt-phosphate (Co-Pi) catalyst on hematite photoanodes for solar water oxidation. *Energy Environ Sci* 4:1759–1764.
42. Seabold JA, Choi KS (2011) Effect of a cobalt-based oxygen evolution catalyst on the stability and the selectivity of photo-oxidation reactions of a WO_3 photoanode. *Chem Mater* 23:1105–1112.
43. Jeon TH, Choi W, Park H (2011) Cobalt-phosphate complexes catalyze the photoelectrochemical water oxidation of $BiVO_4$ electrodes. *Phys Chem Chem Phys* 13:21392–21401.
44. Wang DE, et al. (2012) Photocatalytic water oxidation on $BiVO_4$ with the electrocatalyst as an oxidation cocatalyst: essential relations between electrocatalyst and photocatalyst. *J Phys Chem C* 116:5082–5089.
45. Pilli SK, et al. (2011) Cobalt-phosphate (Co-Pi) catalyst modified Mo-doped $BiVO_4$ photoelectrodes for solar water oxidation. *Energy Environ Sci* 4:5028–5034.
46. Zhong DK, Choi S, Gamelin DR (2011) Near-complete suppression of surface recombination in solar photoelectrolysis by "Co-Pi" catalyst-modified W:$BiVO_4$. *J Am Chem Soc* 133:18370–18377.
47. Seabold JA, Choi KS (2012) Efficient and stable photo-oxidation of water by a bismuth vanadate photoanode coupled with an iron oxyhydroxide oxygen evolution catalyst. *J Am Chem Soc* 134:2186–2192.
48. Schuhl Y, et al. (1983) Study of mixed-oxide catalysts containing bismuth, vanadium and antimony-preparation, phase-composition, spectroscopic characterization and catalytic-oxidation of propene. *J Chem Soc, Faraday Trans 1* 79:2055–2069.
49. Nefedov VI, Firsov MN, Shaplygin IS (1982) Electronic-structures of $MRhO_2$, MRh_2O_4, $RhMO_4$ and Rh_2MO_6 on the basis of X-Ray spectroscopy and esca data. *J Electron Spectrosc Relat Phenom* 26:65–78.
50. Barbaray B, Contour JP, Mouvier G (1978) Effects of nitrogen-dioxide and water-vapor on oxidation of sulfur-dioxide over V_2O_5 particles. *Environ Sci Technol* 12:1294–1297.
51. Blass PM, Zhou XL, White JM (1990) Coadsorption and reaction of water and potassium on Ag(111). *J Phys Chem* 94:3054–3062.
52. Stec WJ, Vanwazer JR, Proctor WG, Morgan WE (1972) Inner-orbital photoelectron spectroscopy of several pairs of similar phosphorus-compounds. *J Inorg Nucl Chem* 34:1100–1104.
53. Mezentzeff P, Lifshitz Y, Rabalais JW (1990) Compositional and chemical modifications of V_2O_5 and $NaVO_3$ induced by N_2^+ bombardment. *Nucl Instrum Methods Phys Res, Sect B* 44:296–301.
54. Aduru S, Contarini S, Rabalais JW (1986) Electron-stimulated, X-Ray-stimulated, and ion-stimulated decomposition of nitrate salts. *J Phys Chem* 90:1683–1688.
55. Musin RN, Lin MC (1998) Novel bimolecular reactions between NH_3 and HNO_3 in the gas phase. *J Phys Chem A* 102:1808–1814.
56. Pourbaix M (1974) *Atlas of Electrochemical Equilibria in Aqueous Solutions* (National Association of Corrosion Engineers International Cebelcor, Houston, TX), 2nd Ed, p 533.
57. Pourbaix M (1974) *Atlas of Electrochemical Equilibria in Aqueous Solutions* (National Association of Corrosion Engineers International Cebelcor, Houston, TX), 2nd Ed., p 234.